ADVANCES IN ATMOSPHERIC SCIENCES, VOL. 26, NO. 5, 2009, 973–983

A Synergic Algorithm for Retrieval of Aerosol Optical Depth over Land

GUO Jianping*[1,2] (郭建平), XUE Yong[2,3] (薛 勇), CAO Chunxiang[2] (曹春香), ZHANG Hao[2] (张 颢), GUANG Jie[2,4] (光 洁), ZHANG Xiaoye[1] (张小曳), and LI Xiaowen[2] (李小文)

[1] *Centre for Atmosphere Watch and Services, Chinese Academy of Meteorological Sciences, China Meteorological Administration, Beijing* 100081

[2] *State Key Laboratory of Remote Sensing Sciences, Jointly Sponsored by the Institute of Remote Sensing Applications of Chinese Academy of Sciences and Beijing Normal University, Institute of Remote Sensing Applications, Chinese Academy of Sciences, P. O. Box* 9718*, Beijing* 100101

[3] *Department of Computing, London Metropolitan University,* 166-220 *Holloway Road, London* N7 8DB*, UK*

[4] *Graduate University, Chinese Academy of Sciences, Beijing* 100049

(Received 29 November 2007; revised 26 November 2008)

ABSTRACT

In this paper, a novel algorithm for aerosol optical depth(AOD) retrieval with a 1 km spatial resolution over land is presented using the Advanced Along Track Scanning Radiometer (AATSR) dual-view capability at 0.55, 0.66 and 0.87 μm, in combination with the Bi-directional Reflectance Distribution Function (BRDF) model, a product of the Moderate Resolution Imaging Spectroradiometer (MODIS). The BRDF characteristics of the land surface, i.e. prior input parameters for this algorithm, are computed by extracting the geometrical information from AATSR and reducing the kernels from the MODIS BRDF/Albedo Model Parameters Product. Finally, AOD, with a 1 km resolution at 0.55, 0.66 and 0.87 μm for the forward and nadir views of AATSR, can be simultaneously obtained.

Extensive validations of AOD derived from AATSR during the period from August 2005 to July 2006 in Beijing and its surrounding area, against *in-situ* AErosol RObotic NETwork (AERONET) measurements, were performed. The AOD difference between the retrievals from the forward and nadir views of AATSR was less than 5.72%, 1.9% and 13.7%, respectively. Meanwhile, it was found that the AATSR retrievals using the synergic algorithm developed in this paper are more favorable than those by assuming a Lambert surface, for the coefficient of determination between AATSR derived AOD and AERONET mearured AOD, decreased by 15.5% and 18.5%, compared to those derived by the synergic algorithm. This further suggests that the synergic algorithm can be potentially used in climate change and air quality monitoring.

Key words: Advanced Along Track Scanning Radiometer, AOD, Bi-directional Reflectance Distribution Function, AERONET

Citation: Guo, J. P., Y. Xue, C. X. Cao, H. Zhang, J. Guang, X. Y. Zhang, and X. W. Li, 2009: A synergic algorithm for retrieval of aerosol optical depth over land. *Adv. Atmos. Sci.*, **26**(5), 973–983, doi: 10.1007/s00376-009-7218-4.

1. Introduction

Aerosols exhibit large spatio-temporal variations on both regional and global scales due to their diverse sources and complicated compositions. The meteorological conditions further alter the distribution and lifespan of aerosols, even resulting in aerosol plumes transported across thousands of miles.

Currently, aerosol properties have widely been determined by ground-based measurements, which are

*Corresponding author: GUO Jianping, jpguo@cams.cma.gov.cn

restricted to small spatial coverage. For example, based on observational data for dust-carried elements in aerosol particles of different deserts, loess and inland regions of China, the sources, transport and deposition of Asian dust were determined (Zhang et al., 1993; Zhang and An, 1997).

However, monitoring air quality on regional scales requires heterogeneous aerosol data that are often prohibitively expensive to acquire by ground-based measurements, although it can be used to characterize the relationship between size distribution, temporal variation of atmospheric aerosols, relative humidity and the Richardson number (Zhang et al., 2001). As a result, satellite-based remote sensing has become an alternative powerful tool.

Taking the limitation of ground-based measurements into account, the application of various spaceborne data in deriving aerosol properties has been attempted since 1965 (Rozenberg et al., 1965), hence diverse algorithms have been presented to retrieve aerosols from satellite data in the last few years (King et al., 1999).

In reality, the atmospheric radiation field is affected by surface reflection from the underlying medium; thereby most aerosol retrieval algorithms over land require homogenous and dark surfaces, like a body of water or dense dark vegetation. The algorithm adopted operationally by the National Aeronautics and Space Administration (NASA) is the Dense Dark Vegetation (DDV) technique (Kaufman et al., 1997; Remer et al., 2005), which only holds true for land surfaces with a low reflectance. The retrieval accuracy is claimed to be $\Delta\tau = \pm 0.05 \pm 0.15\tau$ with a 10-km resolution (τ denotes aerosol optical depth, namely AOD). However, the Moderate Resolution Imaging Spectroradiometer (MODIS) AOD product cannot discriminate dense haze, and tends to be inaccurate over land with high reflectance or snow cover (Engel-Cox et al., 2004). Furthermore, Wang et al. (2007) demonstrated that the MODIS aerosol products lacked universal applicability over China, due to extensive spatial coverage, the heterogeneity of the land surface and various aerosol models in different regions. Fortunately, the DEEP BLUE algorithm developed by Hsu et al. (2004) can be used to derive aerosol optical properties over bright targets like bright urban areas and deserts, which serve as separate and complementary parameters to the MYD04 aerosol product.

Owing to the high reflectance and heterogeneity of the underlying surface and the high spatio-temporal variation of aerosols suspended in the air, AOD retrieval over land, particularly over high reflective land, remains a challenge. Attempts at retrieving AOD over high reflective land have continued, such as the Contrast Reduction method (Tanré et al., 1988), which made the assumption of invariability of the land surface reflectance during the time interval of two different satellite images. Tang et al. (2005) developed a novel AOD retrieval method especially for bright land surfaces, by exploiting the synergy of the Terra and Aqua MODIS data, in which the assumption should be made of the invariance of both the wavelength exponent of the aerosols and the bidirectional surface reflectance during the time intervals between Terra and Aqua overpasses. Liang et al. (2006) developed an improved aerosol estimation algorithm from MODIS based on a sequence of imagery over land surfaces, especially "bright surfaces" within a period of time, in terms of the assumption that surface properties are relatively stable and atmospheric conditions vary dramatically.

In contrast to single-view sensors and their shortcomings and limitations, multi-angle imaging radiometers offer the potential to improve the separation of scattering and attenuation from land surfaces (North et al., 1999). This indeed, would improve the retrieval accuracy of aerosol loading. Attempts at using such radiometers have been ongoing since the 1990s. Multi-angle satellite radiometry was first used by Martonchik and Diner (1992). Later, dual-view data from the Along Track Scanning Radiometer 2 (ATSR-2) were employed to retrieve aerosol optical properties (Floweredew and Haigh, 1995; North et al., 1999; Veefkind et al., 2000). The Advanced Along Track Scanning Radiometer (AATSR), the immediate successor to ATSR-2, was also applied successfully (Grey et al., 2006). Other novel multi-angle sensors, such as the Multi-angle Imaging SpectroRadiometer (MISR) (Diner et al., 2001; Kahn et al., 2001) and the Polarization and Directionality of Earth's Reflectance (POLDER) sensor (Deuzé et al., 1999), are being used as well.

There exist diverse problems in all the above-mentioned algorithms, resulting in a low accuracy of the derived AOD. Therefore, accounting for the full coupling between the land surface Bi-directional Reflectance Distribution Function （BRDF） and the atmospheric scattering has been shown to be important (Vermote, 1997), and may be a potential alternative to enhance the inversion accuracy.

As an attempt to retrieve AOD over land, in this paper we proposed a synergic algorithm to retrieve AOD over land using the dual-angle measurements of AATSR, in conjunction with separate BRDF characteristics of the underlying land surface from the MODIS BRDF product. The text below is organized as follows. In section 2, a brief discussion of the algorithm's physical basis is presented, followed by a description of the retrieval algorithm to derive AOD.

The linear semi-empirical kernel-driven BRDF model is introduced as well, in order to derive AOD from AATSR data by coupling the Earth-atmosphere system. Various data used in this work and the retrieval experiments are described in section 3. Validations of AOD at 0.55, 0.66 and 0.87 μm of AATSR acquired during the period August 2005 to July 2006 over Beijing and its surrounding area were performed against AERONET measurements in section 4. Intercomparison between AOD from the synergic algorithm developed in this paper and that by assuming a Lambertian surface was done as well in this section. Section 5 draws some preliminary conclusions and develops a proposal for future work.

2. Algorithm

A key problem in aerosol retrieval is to distinguish between surface and atmospheric contributions to signals observed by satellite sensors. A major contribution in the surface-related variability is due to the non-Lambertian nature of the Earth's surface reflectance and the fact that for a polar orbiting sensor, the illumination/observation geometry varies considerably between successive observations of the same area.

The top of the atmosphere (TOA) angular spectral reflectance at a wavelength results from: scattering of radiation within the atmosphere without interaction with the surface (known as the "atmospheric path reflectance"), the reflection of radiation off the surface that is directly transmitted to the TOA (the "surface function"), and the reflection of radiation from outside the sensor's field of view (the "environment function"). The environment function is neglected. Therefore, a common method for determining the atmospheric contribution to the satellite signal is to make an assumption about the surface reflectivity or albedo (Borde and Verdebout, 2003).

Moreover, the signals onboard satellites definitely contain information from both the surface properties and the atmospheric constituents. It remains an ill-poised problem, and in order to solve it, various mathematical algorithms have been developed to decouple them successfully (King et al., 1999).

The present study is rather undertaken to prospect the possibilities of retrieving the AOD over land by coupling the MODIS BRDF parameter product and the AATSR bi-angular TOA radiance measurements, through solving the traditional integrodifferential radioactive transfer equation developed by Chandrasekhar (1960). Based on the general solution to this equation given by Kontratyev (1969), and under the assumption of no thermal radiation and a plane-parallel atmosphere, Xue and Cracknell (1995) proposed a formula describing the relation between the ground surface reflectance A and the TOA reflectance A', as shown in Eq. (1).

$$A = \frac{(A'b - a) + a(1 - A')e^{(a-b)\xi\tau_0^{\lambda}\sec\theta'}}{(A'b - a) + b(1 - A')e^{(a-b)\xi\tau_0^{\lambda}\sec\theta'}}\ , \qquad (1)$$

where $a = \sec\theta$ and $b = 2$, ξ is the backscattering coefficient, typically 0.1. The atmospheric optical depth mainly consists of the molecular Rayleigh scattering and the aerosol scattering.

The simplest way to examine the spectral dependence of aerosol particles is implemented by using the Angstrom power law given by

$$\tau_a = \beta\lambda^{-\alpha}\ , \qquad (2)$$

where α is the wavelength exponent, β is the turbidity parameter and λ is the wavelength (Angstrom, 1964; Shaw et al., 1973). The value of α depends on the ratio of the concentration of large to small aerosols and β represents the total aerosol loading in the atmosphere, which primarily depends on the large particle abundance. The values of α and β are obtained by the least square fit of the spectral optical depths on a log-log scale.

For the molecular Rayleigh scattering $\tau_{M,\lambda}(\infty)$, Linke (1956) has given an approximate expression, which is sufficiently accurate for most applications in remote sensing as follows (next page):

$$\tau_{M,\lambda}(\infty) = 0.00897\lambda^{-4.09}. \qquad (3)$$

Therefore the total extinction in the whole atmospheric column can be described as

$$\tau_0 = \tau_a + \tau_M = \beta\lambda^{-\alpha} + 0.00897\lambda^{-4.09}. \qquad (4)$$

Meanwhile, an assumption should be made of the invariance of the wavelength exponent α throughout about 2 minute intervals between the nadir and forward views of AATSR to the same surface target.

Now, if we substitute dual-angle AATSR 2 visible spectral bands, centered at wavelengths of 0.55, 0.66 and 0.87 μm, respectively, into Eq. (1), we can obtain 6 nonlinear equations as follows:

$$A_{\mathrm{N},\lambda_i} = \frac{(A'_{\mathrm{N},\lambda_i}b - a_{\mathrm{N}}) + a_{\mathrm{N}}(1 - A'_{\mathrm{N},\lambda_i})e^{(a_{\mathrm{N}}-b)\xi(0.00897\lambda_i^{-4.09}+\beta_{\mathrm{N}}\lambda_i^{-\alpha})}}{(A'_{\mathrm{N},\lambda_i}b - a_{\mathrm{N}}) + b(1 - A'_{\mathrm{N},\lambda_i})e^{(a_{\mathrm{N}}-b)\xi(0.00897\lambda_i^{-4.09}+\beta_{\mathrm{N}}\lambda_i^{-\alpha})}} \qquad (5)$$

$$A_{\mathrm{F},\lambda_i} = \frac{(A'_{\mathrm{F},\lambda_i} b - a_{\mathrm{F}}) + a_{\mathrm{F}}(1 - A'_{\mathrm{F},\lambda_i}) e^{(a_{\mathrm{F}}-b)\xi(0.00897\lambda_i^{-4.09}+\beta_{\mathrm{F}}\lambda_i^{-\alpha})\sec(\frac{55}{180}\pi)}}{(A'_{\mathrm{F},\lambda_i} b - a_{\mathrm{F}}) + b(1 - A'_{\mathrm{F},\lambda_i}) e^{(a_{\mathrm{F}}-b)\xi(0.00897\lambda_i^{-4.09}+\beta_{\mathrm{F}}\lambda_i^{-\alpha})\sec(\frac{55}{180}\pi)}} \tag{6}$$

where A_{N,λ_i}, A_{F,λ_i} respectively stand for the observation of the nadir and forward views; i=1, 2, 3 respectively stand for the visible/near infrared wavelengths centered at 0.55, 0.66 and 0.87 μm, respectively. $a_{\mathrm{N}} = \sec 0 = 1$, $a_{\mathrm{F}} = \sec \pi 55/180$ and $b = 2$ (the upward traveling radiation can be considered as isotropic scattering at a first approximation of scattering, if particular situations with specular reflection are excluded).

It is very difficult to simultaneously retrieve AOD at 0.55, 0.66 and 0.87 μm since a single AATSR measurement with 3 wavelengths and dual views corresponds to 6 equations with 9 unknowns (that is A_{N,λ_1}, A_{N,λ_2}, A_{N,λ_3}, A_{F,λ_1}, A_{F,λ_2}, A_{F,λ_3}, β_{F}, β_{N}, and α), which is a typical ill-posed inversion problem. Without any *a priori* information, it is almost impossible for us to analytically derive the unknown parameters from Eqs. (5) and (6). Flowerdew and Haigh (1995), however, assumed that the ratio of 'dual angle' surface reflectance depends only on the geometry of measurements of the satellite sensor and is independent of the wavelength, which is formulated as follows:

$$k = \frac{A_{\mathrm{F}}}{A_{\mathrm{N}}} \tag{7}$$

where k represents the ratio of the forward view to the nadir view reflectance, and k is independent of the wavelength. Using the geometrical conditions of AATSR, combined with the MODIS BRDF product, the reflectance can be reduced using the linear kernel-driven BRDF model (Roujean et al., 1992) as follows:

$$\begin{aligned} R(\theta_s, \theta_v, \phi, \lambda_i) =& f_{\mathrm{iso}}(\lambda_i) + f_{\mathrm{vol}}(\lambda_i) K_{\mathrm{vol}}(\theta_s, \theta_v, \phi) + \\ & f_{\mathrm{geo}}(\lambda_i) K_{\mathrm{geo}}(\theta_s, \theta_v, \phi) \end{aligned} \tag{8}$$

where $f_{\mathrm{iso}}(\lambda_i)$, $f_{\mathrm{vol}}(\lambda_i)$ and $f_{\mathrm{geo}}(\lambda_i)$ represent the parameters extracted from the MODIS BRDF product, $K_{\mathrm{geo}}(\theta_s, \theta_v, \phi)$ and $K_{\mathrm{vol}}(\theta_s, \theta_v, \phi)$ are the RossThick and the LiSparse kernels, respectively. The first, second and third term of the right hand in Eq. (8) represent isotropic, volumetric scattering, and geometric scattering contribution from surface, respectively. The full derivations can be found in (Wanner et al., 1995). Here, kernels can be described as a function of the collocated AATSR geometry.

Meanwhile, by assuming the BRDF of the land surface to be constant during the time intervals between MODIS and AATSR overpasses, the k value mainly derived from Eq. (8) is equal to that derived from AATSR, as formulated with Eq. (9).

$$\frac{A_{\mathrm{F},\lambda_i}}{A_{\mathrm{N},\lambda_i}} = k = \frac{R_{\mathrm{F}}}{R_{\mathrm{N}}} \tag{9}$$

This relationship may be exploited directly to give a constraint for AOD retrieval by forcing the retrieved bidirectional reflectance to have a consistent angular variation across the wavebands specified, even though the magnitude of the reflectance may vary greatly. Now the formidable equation can be solved by numerical approximation based on the Broyden iterative method (Broyden, 1965; William, 1992), thus simultaneously retrieving AOD at 0.55, 0.66 and 0.87 μm of the AATSR forward view and nadir view, respectively.

3. Data and experiment

Due to the algorithm first proposed here, as many as possible AATSR observations, in conjunction with *in-situ* AERONET data, are required as long as possible. In our work, one year of AATSR observations, MODIS BRDF/Albedo Model Parameters Product and coincident *in-situ* AERONET data during the period from August 2005 to July 2006 were collected, which covered Beijing, China and its surrounding area. Experiments were carried out using the abovementioned data to validate the algorithm as well. Furthermore, the validation methods and results will be described in detail in section 4. While the data required in the algorithm developed in this paper will be expounded on as follows.

3.1 *AATSR data*

The AATSR conical scan allows two successive observations to be made of the same land surface within about a 2-minute interval, by measuring the radiance at approximately the nadir and 55° forward (along-track) views. The instantaneous field of view (IFOV) is approximately 1 km for the nadir view and 4 km for the forward view, with a swath width of 500 km (nadir). AATSR has three visible channels centered at 0.55, 0.66 and 0.87 μm, intended for applications in AOD retrieval experiments used in this study.

The MODIS BRDF/Albedo Model Parameters Product has the temporal cycle of 16 days, and it assumes the BRDF to be consistent during the cycle.

3.2 *MODIS BRDF/Albedo Model Parameters Product*

The MOD43B1 BRDF/Albedo Model Parameters Product can provide parameters required for the RossThickLiSparse Reciprocal BRDF model [shown in Eq. (8) as well] taken in this study at 1 km spatial resolution on a 16-day cycle. In order to georeference the MOD43B1 parameter product to the AATSR data,

the product consistent with AATSR acquired for the same time period August 2005 to July 2006 is selected, assuming the invariability of the BRDF shape during the 16-day time period. Allowing for Eq. (9), 24 total sets of parameters at 0.55 μm can be directly used in a forward model of the BRDF formulation in Eq. (8) for all specified wavelengths.

3.3 *AERONET*

AERONET (AErosol RObotic NETwork) is a federated optical ground-based aerosol monitoring network and data archive supported by NASA's Earth Observing System and expanded by federation with many non-NASA institutions distributed over land and ocean around the world, which measures the aerosol properties over land and ocean throughout the world at 0.34, 0.38, 0.44, 0.50, 0.67, 0.87 and 1.02 μm, respectively. Moreover, the network imposes standardization of instruments, calibration and processing (Holben et al., 1998). The highest-level product (level 2.0), which is cloud-screened (Smirnov et al., 2000) and quality assured with an estimated accuracy of 0.01–0.02 (Eck et al., 1999), was used in validations against AOD retrievals from AATSR measurements in this study.

3.4 *Retrieval experiment*

The AATSR satellite images covering the same spatial range of 38.00°–41.04°N and 114.42°–117.46°E were acquired for the time period August 2005 to July 2006. Owing to the requirements of co-registration between the AATSR and MODIS BRDF/Albedo Model Parameters Product with a 16-day temporal resolution, the number of AATSR images amounts to 24. The following atmospheric conditions like haze, dust and clear sky were meanwhile, taken into account as well in selecting AATSR to validate the algorithm developed in section 2. The co-located ground-based AERONET level 2.0 aerosol measurements for the same period over the study area should be obtained as well.

Due to the fact that the algorithm is not suitable for cloud-contaminated pixels, the first step in the retrieval of AOD by combining the AATSR and BRDF/Albedo Model Parameters Product was to screen out the cloud-contaminated pixels by using the screening method developed by Stowe (1991). The algorithm was then applied to the TOA reflectance data from the forward and nadir views of AATSR, respectively.

BRDF values were calculated by the RossThick-LiSparse Reciprocal BRDF model [c.f. Eq. (8)], in which the parameters were extracted from the MOD43B1 BRDF/Albedo Model Parameters Product, and kernel values were estimated from geometrical information of AATSR. Then, by combining the reflectance, geometry information from the AATSR measurements and BRDF from the MODIS BRDF/Albedo Model Parameters products, based on the algorithm described in section 2, the AOD can be retrieved successfully.

Meanwhile, to testify the importance of the coupling of the surface BRDF and atmospheric scattering in this algorithm, AOD retrievals by assuming the underlying surface to be Lambert were performed as well, which was implemented simply by assigning unity to k of Eq. (9). Furthermore, inter-comparisons between them were made as well.

4. Results and validation

In this section, we will mainly present the results of the AOD retrieval experiment on the basis upon one year (i.e. August 2005 to July 2006) of comparisons between 1 km resolution AOD derived from AATSR in conjunction with the MODIS BRDF product and *in-situ* measurements obtained during the same time period from AERONET data at the Beijing site.

4.1 *Validation against AERONET*

As a rule, the validation of satellite derived geophysical products is difficult because satellite observations cover much larger areas than *in-situ* measurements (Lucht et al., 2000). A key problem arising from such different measurement scales is whether a single ground measurement represents the mean value for a pixel at the satellite scale (Tian et al., 2002). Anywhere, accounting for the heterogeneity of the underlying land surface and the need to reduce the uncertainty induced by the dual-angle geometry of AATSR, we averaged AOD over a 3×3 pixel region, centered at the Beijing AERONET site to reduce noise and minimize the effect of co-registration errors between the nadir and forward observations of the AATSR instrument.

As for the temporal domain of validation, since the AERONET sun photometer samples the direct and sky radiance at different wavelengths from AATSR, in order to compare AERONET and AATSR retrieved AOD, the AERONET AOD of the 24 days consistent with AATSR acquirements at Beijing (39.98°N, 116.38°E) have to be determined at wavelengths of 0.55, 0.66 and 0.87 μm, respectively. Here a second order polynomial fit in the logarithm of wavelength was applied, which was thought as an effective tool for the majority of validation studies (e.g., Ignatov et al., 1995; Knapp and Stowe, 2002). Furthermore, to make

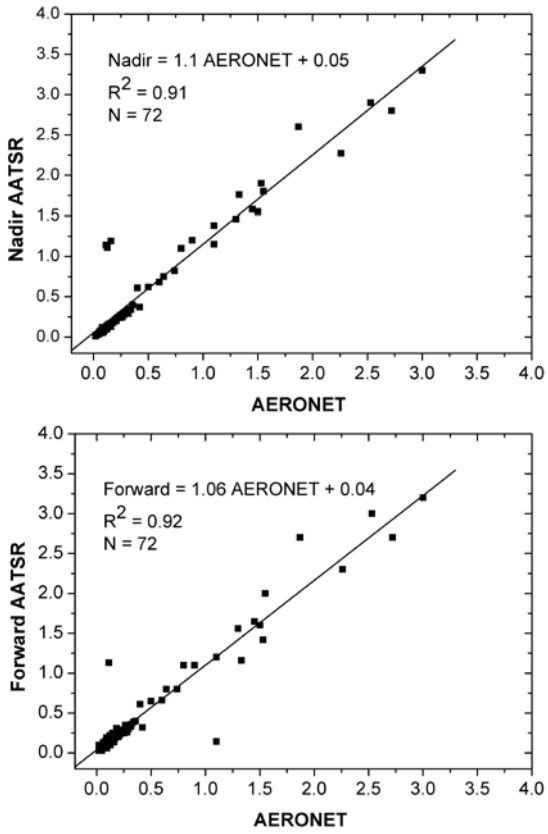

Fig. 1. Scattergrams of AERONET AOD at the Beijing site (39.98°N, 116.38°E) in relation to AOD retrieved from co-located nadir view measurements of AATSR (upper panel), forward view measurements of AATSR (lower panel), respectively. The black line means the fitted linear regression curve (the wavelengths of 0.55, 0.67 and 0.87 μm are all included).

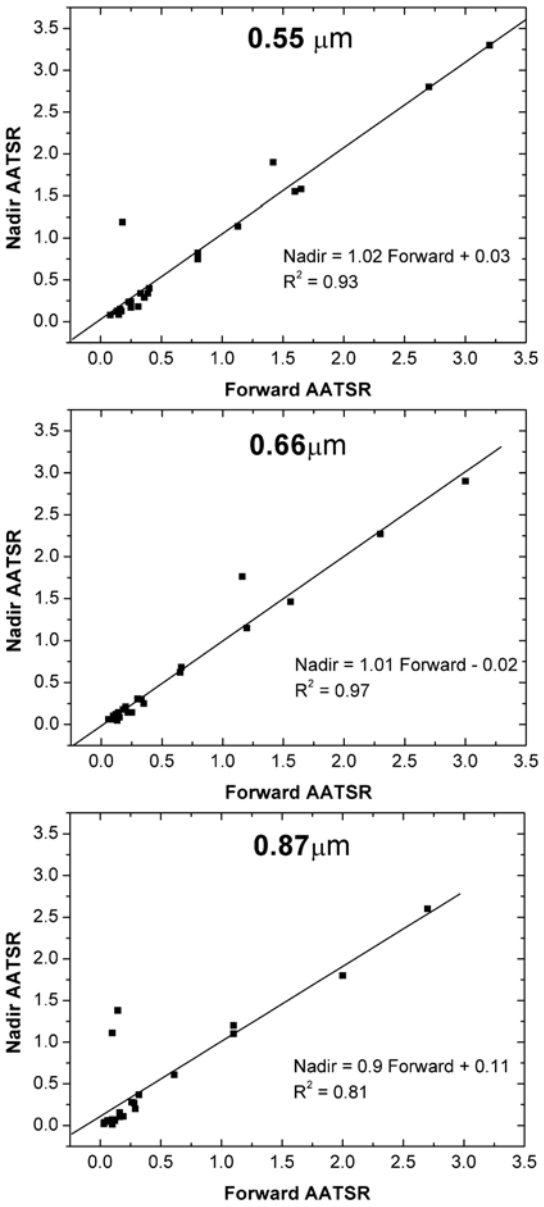

Fig. 2. Scattergrams of AOD retrieved from the nadir AATSR in relation to those from the forward AATSR at 0.55, 0.66 and 0.87 μm over Beijing (region of 3×3 pixel), respectively. The black line represents the fitted linear regression curve.

sure that they were co-located in the temporal domain with each other, AERONET data were averaged using measurements observed within 30 minutes of the AATSR overpass, which implied that the AATSR images without AERONET observations falling within 30 minutes of the AATSR overpass cannot be selected for validations. The requirements of the temporal frequency of AERONET reduced the number of AATSR available for validations, accounting for why 24 images, in some degree, were selected during a year period.

The intercomparisons of AOD were based upon the 144 measurements at the collocated AERONET Beijing site for the 24 days. Figure 1 showed scattergrams of the AERONET AOD at Beijing (39.98°N, 116.38°E) in relation to AOD retrieved from the co-located nadir view measurements of AATSR and the forward view measurements of AATSR, respectively. Significant correlation was found with a determinant coefficient of 0.91 and 0.92 for the nadir view and forward view of AATSR, respectively. The AOD difference (defined as $|(\mathrm{Mean}_{\lambda_i,\mathrm{Forward}} - \mathrm{Mean}_{\lambda_i,\mathrm{Nadir}}) \times 100/\mathrm{Mean}_{\lambda_i,\mathrm{Nadir}}|\%$, where $\mathrm{Mean}_{\lambda_i,\mathrm{Forward}}$ denotes mean value of AOD derived at forward view at wavelength λ_i, while $\mathrm{Mean}_{\lambda_i,\mathrm{Nadir}}$ for mean value of AOD at nadir view at wavelength λ_i) between the dual views of AATSR at 0.55, 0.66 and 0.87 μm, is less than 5.72%, 1.9% and 13.7%, respectively. This demonstrates that high consistency exists between AOD retrieved from the forward and nadir views of AATSR, respectively, largely due to the fact that the AOD from the forward

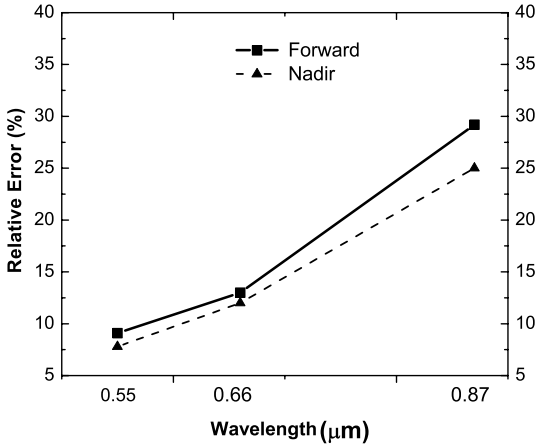

Fig. 3. Relative error of AOD retrieved from the forward (solid square) and nadir views (solid triangle) of AATSR, respectively, as a function of wavelength.

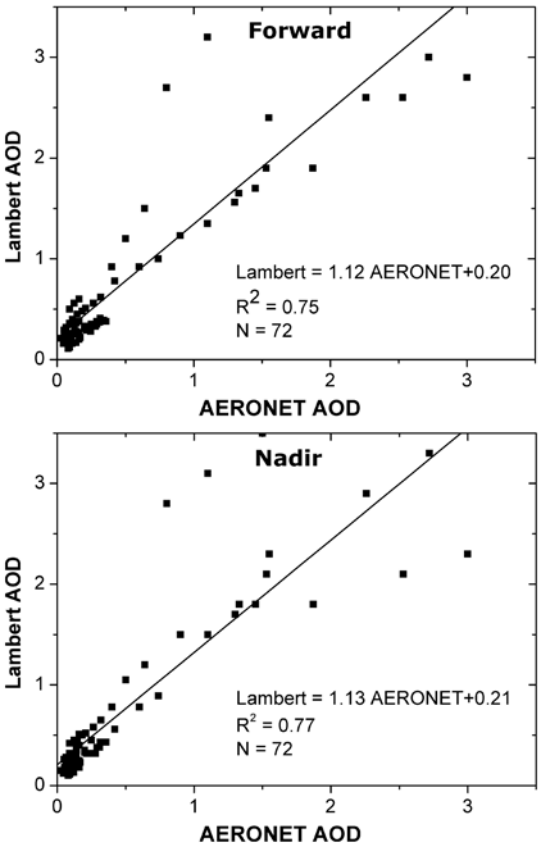

Fig. 4. Scattergrams of AERONET AOD at the Beijing site (39.98°N, 116.38°E) in relation to the Lambert AOD retrieved from the co-located nadir view measurements of AATSR (upper panel), forward view measurements of AATSR (lower panel), respectively. The black line means the fitted linear regression curve (the wavelengths of 0.55, 0.67 and 0.87 μm are all included).

AATSR has been normalized by $\sec\frac{\pi 55}{180}$, as shown in Eq. (6).

There exists strong correlation between AOD from the forward and nadir views of AATSR at 0.55, 0.66 and 0.87 μm, respectively, as clearly shown in Fig. 2.

The averaged relative error of AOD retrieved from dual views of the AATSR images increased with the increasing wavelength, as illustrated in Fig. 3. It is showed in Fig. 3 that the averaged relative error at 0.55, 0.66 and 0.87 μm of the nadir view of AATSR is 7.8%, 12%, and 25%, respectively, while 9.1%, 13%, and 29.2%, respectively, for the forward view. The accuracy at the visible wavelength of 0.55 and 0.66 μm are, therefore, much better than that in the near infrared wavelength, and the nadir and forward view AATSR were comparative in the retrieval accuracy of AOD.

4.2 *Comparison with Lambertian surface derived AOD*

If we substitute 1 into k on the left side of Eq. (7), which means that the surface is assumed to be Lambert and the reflectance is constant and independent of different view angles, AOD can as well be retrieved in the same channels as the synergic algorithm described in section 2.

To prove the sensitivity of the synergic algorithm to the land surface, AOD was derived by assuming the surface to be Lambert using the same data set as the synergic algorithm, with other requirements invariable.

The following points were obvious from Fig. 4, in which ground-based AERONET AOD measurements are compared with those derived from the forward and nadir view of AATSR, respectively, in the case of a Lambert surface assumption. On one hand, the AATSR retrievals using the synergic algorithm developed in this paper were more favorable than those by assuming a Lambert surface, for the coefficient of determination decreased by 15.5% and 18.5% at the nadir and forward view, respectively, compared with Fig. 2, which to some extent demands for taking account of the BRDF characteristics of the land surface. On the other hand, the Lambert AOD is significantly correlated with *in-situ* measurements as well.

4.3 *Regional mapping: A case study*

Due to the importance of regional AATSR AOD retrievals in assessing the regional radiative impact of aerosols based on a climate model, we should map the regional distribution of AOD.

To investigate the potential of the synergic algorithm of mapping the AOD distribution on a regional scale, we took AATSR satellite images acquired at

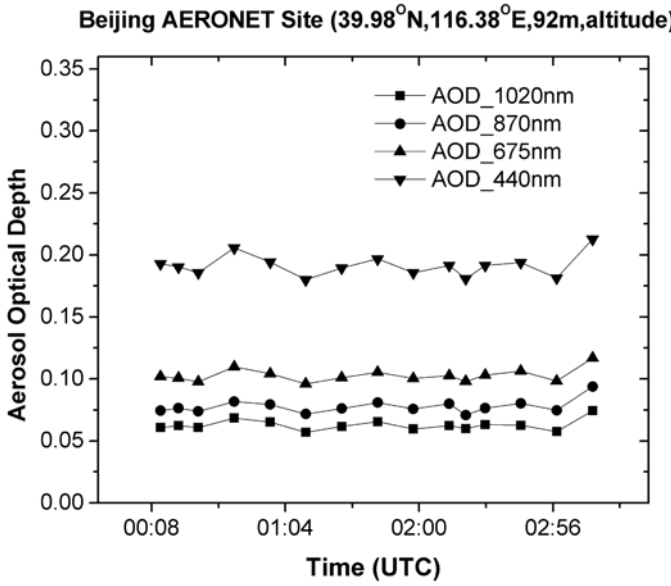

Fig. 5. Ground-based AOD measurements at different wavelengths at the Beijing AERONET site, as a function of time (UTC) on 28 May 2006.

0242 UTC on 28 May 2006 as an example for *in-situ* AERONET AOD, which varied little during the time period of AATSR overpass (shown in Fig. 5).

Regional AOD retrievals were conducted by assuming the land surface to be Lambert (as shown in Figs. 6a, c, e) and taking into account the BRDF of the land surface as well (as shown in Figs. 6b, d, f).

The spatial distribution of AOD in this study area is shown in Fig. 4, in which most AODs in the right panel of Fig. 4 are more explicitly depicted other than the left panel. The retrieved AODs (shown in the right panel of Fig. 4) from the synergic algorithm at the lower right corner (corresponding to the North China plain) of the study area at 0.55, 0.66 and 0.87 μm of AATSR, for example, were higher than that in the left panel, which otherwise was retrieved by assuming the land surface to be Lambert. Moreover, in the upper left corner (corresponding to the mountainous area), there exist higher AOD values in the right panel than the left one. i.e., the synergic algorithm can capture more aerosol information, compared with not considering the BRDF characteristics of the land surface. Therefore, the BRDF characteristic of the land surface cannot be ignored in the retrieval of AOD over land, especial over heterogeneous areas. Furthermore, the Lambertian assumption of the land surface in mountainous areas is not acceptable at a 1 km spatial resolution scale.

It can be obviously seen from Fig. 6 that the AOD value decreases with an increased wavelength. Meanwhile, the spectral variation of AOD is consistent with the characteristics of an anthropogenic source of the aerosols, indicating that the anthropogenic activity can largely attribute to aerosol plumes in this area. The aerosol optical depth as well as its spectral dependence shows large spatial variations over a comparatively small spatial scale over the Beijing area. The majority of AOD (a matter of 75%) in the study area of this case is lower than 0.39, even AOD in some areas cannot be available, basically consistent with the actual *in-situ* measurements.

5. Conclusion

A synergic aerosol retrieval method is presented in this paper that takes advantage of the wide spectral range and the dual-view capability of AATSR for AOD retrieval over land by combining the BRDF characteristics of the land surface. Through one year of AATSR retrieval validation against *in-situ* AERONET measurements, the following conclusion can be drawn:

(1) The accuracy of AOD retrieved from the forward and nadir views of AATSR were comparative, since the AOD difference between the dual views of AATSR at 0.55, 0.66 and 0.87 μm was less than 5.72%, 1.9% and 13.7%, respectively.

(2) In the visible channels (0.55, 0.66 and 0.87 μm) of AATSR, a favorable agreement between the retrieved AOD from AATSR and the collocated ground-based AERONET data was achieved for the forward and nadir views, with a coefficient of determination of 0.91 and 0.92 for the nadir view and the forward view

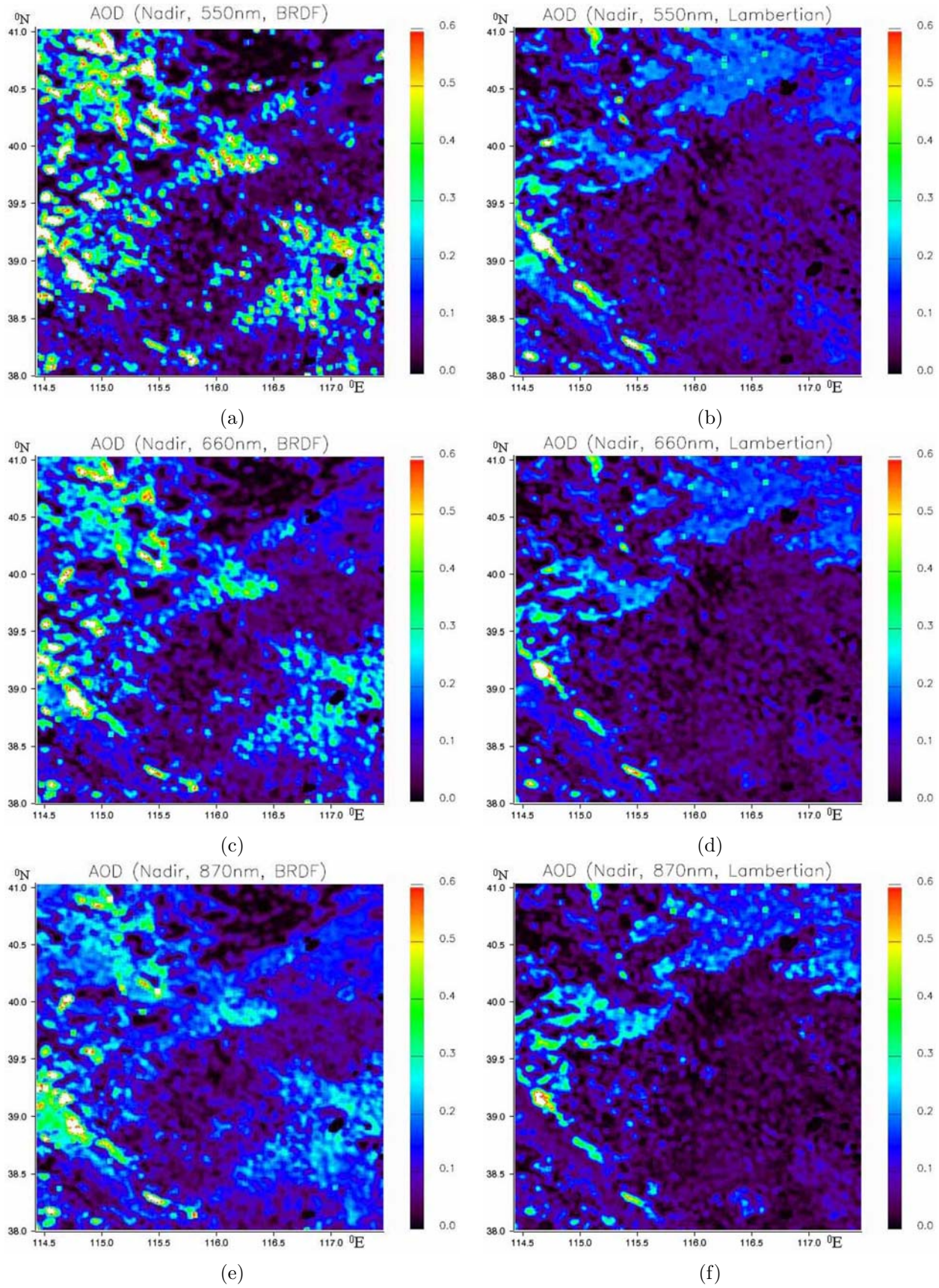

Fig. 6. AOD regional distributions on 28 May 2006 retrieved by the synergic algorithm (a, c, e), in comparison with those retrieved by assuming a Lambertian land surface (b, d, f).

of AATSR, respectively, demonstrating that the synergic algorithm developed in this paper can potentially be applied over land.

(3) It was found that the AATSR retrievals using the synergic algorithm developed in this paper are more favorable than those by assuming a Lambert surface, for the coefficient of determination decreased by 15.5% and 18.5%, compared to those derived by the synergic algorithm. Understanding well the angular dependencies of the retrieved AOD, therefore, will probably enhance the accuracy of AOD retrieval from satellite measurements.

Of course, further validation in different surface conditions and atmospheric regimes with sufficient long period statistics is needed in the near future. Furthermore, the accuracy of the AATSR retrievals and the experiment of AOD mapping conducted on a regional scale, using the synergic algorithm suggest that the synergic algorithm can potentially be used to help narrow the uncertainties associated with aerosol radioactive forcing of the global climate.

Acknowledgements. This publication is an output from the research projects entitled "Study on the National AOD Retrieval System based on MODIS Data" supported by the Special Funds for the Basic Research in Chinese Academy of Meteorological Sciences (CAMS) of Chinese Meteorological Administration (CMA) (2007Y001), "Multi-scale Aerosol Optical Thickness Quantitative Retrieval from Remotely Sensing Data at Urban Area" (40671142) and the project (Grant Nos. 40871173, 40601068) funded by National Natural Science Foundation of China, Innovation Fund by State Key Laboratory of Remote Sensing Sciences, Institute of Remote Sensing Applications of Chinese Academy of Sciences (Grant Nos. 07S00502CX, 03Q0033049), and "Aerosol over China and Their Climate Effect" supported by National Basic Research Program of China (2006CB403701). Thanks will go to European Space Agency (ESA) for providing the AATSR data and to NASA as well for providing the MODIS product free of charge. The PIs of The Beijing AERONET site are also appreciated for collecting the aerosol measurements.

REFERENCES

Angstrom, A., 1964: Techniques of determining the turbidity of the atmosphere. *Tellus*, **13**, 214.

Borde, R., and J. Verdebout, 2003: Remote sensing of aerosols optical thickness over various sites using SeaWiFs or VEGETATION and ground measurements. *Remote Sens. Environ.*, **86**, 42–51.

Broyden, C. G., 1965: A class of methods for solving nonlinear simultaneous equations. *Mathematics of Computation*, **19**, 577–593.

Chandrasekhar, S., 1960: *Radiative Transfer*. New York, Dover Publication, Inc., New York, 393pp.

Deuzé, J. L., M. Herman, P. Goloub, D. Tanré, and A. Marchand, 1999: Characterization of aerosols over ocean from POLDER/ADEOS-1. *J. Geophys. Res.*, **26**, 1421–1424.

Diner, D. J., and Coauthors, 2001: MISR aerosol retrievals over southern Africa during the SAFARI-2000 dry season campaign. *Geophys. Res. Lett.*, **28**, 3127–3130.

Eck, T., B. Holben, J. Reid, O. Dubovik, A. Smirnov, N. O'Neill, I. Slutsker, and S. Kinne, 1999: Wavelength dependence of optical depth of biomass burning, urban, and desert dust aerosols. *J. Geophys. Res.*, **104**, 31333–31349.

Engel-Cox, J. A., C. H. Holloman, B. W. Coutant, and R. M. Hoff, 2004: Qualitative and quantitative evaluation of MODIS satellite sensor data for regional and urban scale air quality. *Atmos. Environ.*, **38**, 2495–2509.

Flowerdew, R., and J. Haigh, 1995: An approximation to improve accuracy in the derivation of surface reflectances from multi-look satellite radiometers. *Geophys. Res. Lett.*, **22**(13), 1693–1696.

Grey, W. M. F., P. R. J. North, and S. O. Los, 2006: Computationally efficient method for retrieving aerosol optical depth from ATSR-2 and AATSR data. *Appl. Opt.*, **45**, 2786–2795.

Holben, B. N., and Coauthors, 1998: AERONET-A federated instrument network and data archive for aerosol characterization. *Remote Sens. Environ.*, **66**(1), 1–16.

Hsu, N. C., S. C. Tsay, M. D. King, and J. R. Herman, 2004: Aerosol properties over bright reflecting source regions. *IEEE Trans. Geosci. Remote Sens.*, **42**, 557–569.

Ignatov, A. M., L. L. Stowe, S. M. Sakerin, and G. K. Korotaev, 1995: Validation of the NOAA/NESDIS satellite aerosol product over the North Atlantic in 1989. *J. Geophys. Res.*, **100**, 5123–5132.

Kahn, R., P. Banerjee, and D. McDonald, 2001: The sensitivity of multi-angle imaging to natural mixtures of aerosols over ocean. *J. Geophys. Res.*, **106**, 18219–18238.

Kaufman, Y. J., D. Tanré, L. Remer, E. Vermote, A. Chu, and B. N. Holben, 1997: Operational remote sensing of tropospheric aerosol over land from EOS Moderate Resolution Imaging Spectroradiometer. *J. Geophys. Res.*, **102**, 17051–17067.

King, M. D., Y. J. Kaufman, D. Tanré, and T. Nakajima, 1999: Remote sensing of tropospheric aerosol from space: past, present, and future. *Bull. Amer. Meteor. Soc.*, **80**, 2229–2259.

Knapp, K. R., and L. L. Stowe, 2002: Evaluating the potential for retrieving aerosol optical depth over land from AVHRR pathfinder atmosphere data. *J. Atmos. Sci.*, **59**, 279–293.

Kontratyev, K. Ya, 1969: *Radiation in the Atmosphere*. Academic Press, New York, 912pp.

Liang, S., B. Zhong, and H. Fang, 2006: Improved esti-

mation of aerosol optical depth from MODIS imagery over land surfaces. *Remote Sens. Environ.*, **104**, 416–425.

Linke, F., 1956: Die Sonnestrahlung und ihre schwachung in der atmosphere. handbuch der geopgyisk, Bd VIII, herausgeg. von F. Linke F. Moeller, Berlin: Gebr. Borntraeger, kap. **6**, 1942–1956. (in German)

Lucht, W., A. H. Hyman, A. H. Strahler, M. J. Barnsley, P. Hobson, and J. P. Muller, 2000: A comparison of Satellite-derived spectral albedos to groundbased broadband albedo measurements modeled to satellite spatial scale for a semidesert landscape. *Remote Sens. Environ.*, **74**, 850–98.

Martonchik, J. V., and D. J. Diner, 1992: Retrieval of aerosol optical properties from multi-angle satellite imagery. *IEEE Trans. Geosci. Remote Sens.*, **30**(2), 223–230.

North, P. R. J., S. Briggs, S. Plummer, and J. Settle, 1999: Retrieval of land surface bidirectional reflectance and aerosol opacity from ATSR-2 multiangle Imagery. *IEEE Trans. Geosci. Remote Sens.*, **37**, 526–537.

Remer, L. A., and Coauthors, 2005: The MODIS aerosol algorithm, products, and validation. *J. Atmos. Sci.*, **62**, 947–973.

Roujean, J. L., M. Leroy, and P. Y. Deschamps, 1992: A bidirectional reflectance model of the Earth's surface for the correction of remote sensing data. *J. Geophys. Res.*, **97**, 20455–20468.

Rozenberg, G. V., and V. V. Nikolaeva-Tereshkova, 1965: Stratospheric aerosol using measurements from space ship. *Izvestiya Academy of Sciences USSR, Atmospheric and Oceanic Physics*, **1**, 386–394.

Shaw, G. E., J. A. Regan, and B. M. Herman, 1973: Investigations of atmospheric extinction using direct solar radiation measurements made with a multiple wavelength radiometer. *J. Appl. Meteor.*, **12**, 374–380.

Smirnov, A., B. N. Holben, T. F. Eck, O. Dubovik, and I. Slutsker, 2000: Cloud screening and quality control algorithms for the AERONET database. *Remote Sens. Environ.*, **73**, 337–349.

Stowe, L. L., 1991: Cloud and aerosol products at NOAA/NESDIS. *Global and Planetary Change*, **4**, 25–32.

Tang, J. K., Y. Xue, T. Yu, and Y. N. Guan, 2005: AOD Determination by Exploiting the Synergy of TERRA and AQUA MODIS. *Remote Sens. Environ.*, **94**, 327–334.

Tanré, D., C. Devaux, H. Herman, and R. Santer, 1988: Radiative properties of desert aerosols by optical ground-based measurements at solar wavelengths. *J. Geophys. Res.*, **93**, 14223–14231.

Tian, Y., and Coauthors, 2002: Multiscale analysis and validation of the MODIS LAI product I. Uncertainty assessment. *Remote Sens. Environ.*, **83**, 414–430.

Veefkind, J. P., G. de Leeuw, R. B. A. Koelemeijer, and P. Stammes, 2000: Regional distribution of aerosol over land derived from ATSR-2 and GOME data. *Remote Sens. Environ.*, **74**, 377–386.

Vermote, E. F., D. Tanre, J. L. Deuze, M. Herman, and J. J. Morcrette, 1997: Second simulation of the satellite signal in the solar spectrum, 6S: An overview. *IEEE Trans. Geosci. Remote Sens.*, **35**, 675–686.

Wang, L. L., G. R. Liu, J. Y. Xin, Y. S. Wang, Z. Q. Li, and P. C. Wang, 2007: Validation of MODIS aerosol products by CSHNET over China. *Chinese Science Bulletin*, **52**, 1708–1718.

Wanner, W., X. Li, and A. H. Strahler, 1995: On the derivation of kernels for kernel-driven models of bidirectional reflectance. *J. Geophys. Res.*, **100**, 21077–21090.

William, H. P., A. T. Saul, T. V. William, and P. F. Brian, 1992: *Numerical Recipes in C*: *The Art of Scientific Computing*. 2nd ed., Cambridge University Press, 994pp.

Xue, Y., and A. P. Cracknell, 1995: Operational bi-angle approach to retrieve the earth surface albedo from AVHRR data in the visible band. *Int. J. Remote Sens.*, **16**, 417–429.

Zhang, R. J., M. X. Wang, and J. Z. Fu, 2001: Preliminary research on the size distribution of aerosols in Beijing. *Adv. Atmos. Sci.*, **18**(2), 225–230.

Zhang, X. Y., and Z. S. An, 1997: Sources, transport and deposition of Asian dust. *Proceedings of Sixth Chinese Aerosol Conference*, China, 68–73.

Zhang, X. Y., R. Arimoto, Z. S. An, T. Chen, G. Y. Zhang, G. H. Zhu, and X. F. Wang, 1993: Atmospheric trace elements over sources regions for Chinese dust: concentrations, sources and atmospheric deposition on the loess plateau. *Atmos. Environ.*, **27**, 2051–2067.